

Modeling a DFIG Wind Turbine System using PLECS

Dr. John Schönberger
Plexim GmbH
Technoparkstrasse 1
8005 Zürich

December 2008

1 Introduction

Variable speed operation is essential for large wind turbines in order to optimize the energy capture under variable wind speed conditions. Variable speed wind turbines require a power electronic interface converter to permit connection with the grid. The power electronics can be either partially-rated or fully-rated [1]. A popular interface method for large wind turbines that is based on a partially-rated interface is the doubly-fed induction generator (DFIG) system [2]. In the DFIG system, the power electronic interface controls the rotor currents in order to control the electrical torque and thus the rotational speed. Because the power electronics only process the rotor power, which is typically less than 25% of the overall output power, the DFIG offers the advantages of speed control for a reduction in cost and power losses.

This report presents a DFIG wind turbine system that is modeled in PLECS and Simulink. A full electrical model that includes the switching converter implementation for the rotor-side power electronics and a dq model of the induction machine is given. The aerodynamics of the wind turbine and the mechanical dynamics of the induction machine are included to extend the use of the model to simulating system operation under variable wind speed conditions. For longer simulations that include these slower mechanical and wind dynamics, an averaged PWM converter model is presented. The averaged electrical model offers improved simulation speed at the expense of neglecting converter switching detail.

2 Background

2.1 Power in the wind

The mechanical power that can be extracted from a wind turbine is given by

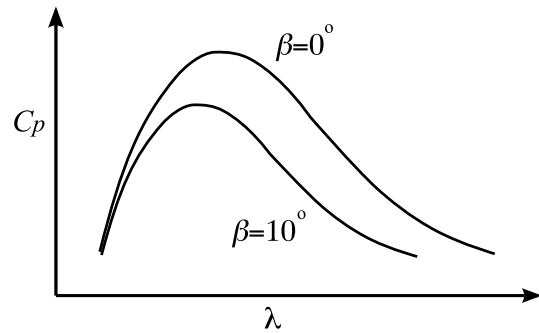


Figure 1: Typical performance coefficient vs. tip speed ratio curve showing the effect of varying the blade pitch angle.

$$P_w = 0.5\rho AC_p v^3 \quad (1)$$

where ρ is the air density, A is the area swept by the turbine blades, C_p is the performance coefficient of the turbine and v is the wind velocity. A typical performance coefficient curve is shown in Fig. 1, where β is the blade pitch angle.

The performance coefficient is dependent on the tip speed ratio, λ , given by

$$\lambda = \frac{\omega_t R}{v} \quad (2)$$

where ω_t is the rotational speed of the turbine and R is the turbine radius. It can be seen that λ should be held constant to harness maximum power from the wind. The turbine rotational speed must therefore increase as the wind speed increases. When the wind turbine reaches its maximum rotational speed however, blade pitch angle control can be employed to shed the excess wind power. Increasing the blade pitch angle decreases the optimum C_p and λ value as shown in Fig. 1.

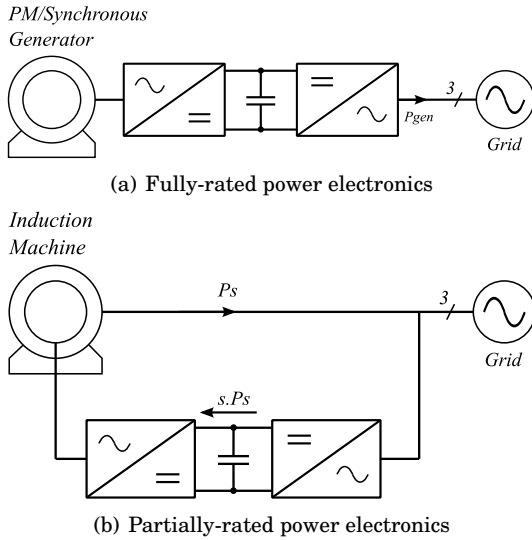


Figure 2: Interface options for wind turbines.

2.2 Types of Wind Turbine Interfaces

Although wind turbine generators can be interfaced directly with the power system, the use of a power electronic interface is preferred since it permits variable speed operation and thus offers increased power extraction from the wind. Variable speed operation also allows wind gusts to be absorbed in the mechanical inertia of the turbine, reducing torque pulsations and fluctuations in the output power.

Power electronic interfaces can be of the fully-rated or partially-rated type as shown in Fig. 2. The fully-rated interface, shown in Fig. 2(a), processes all power produced by the turbine. This type of interface is often used with a permanent magnet generator. The fully-rated interface permits control flexibility over the entire operating range of the wind turbine; however, the converter and EMI filter is costly compared with a partially-rated interface.

The partially-rated interface processes a portion of the power output of the turbine and offers control flexibility over most of the operating range of the wind turbine. A partially-rated interface is typically used with a DFIG where the power electronic interface only processes the rotor power. This scheme is shown in Fig. 2(b). The main advantages of this scheme are a reduction in the size and cost of the interface converter and a consequent reduction in overall converter losses.

2.3 DFIG system

The DFIG is based on a wound-rotor type induction machine. The torque-speed profile of a typical induction machine with a short-circuited rotor is shown in Fig. 3. The induction machine has two operating regions, subsynchronous and supersynchronous, that correspond to rotation below or above

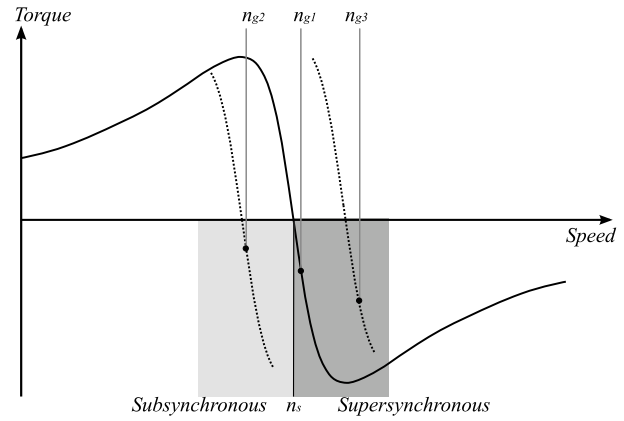


Figure 3: Torque-speed characteristic of induction machine with short-circuited rotor. Rotor current control permits alteration of torque profile in subsynchronous and supersynchronous regions.

the synchronous speed. The synchronous speed of the generator in rpm is defined by

$$n_s = \frac{f}{z_p} \times 60 \quad (3)$$

where f is the grid frequency and z_p is the number of pole pairs. For a 50 Hz generator with two pole pairs, $n_s = 1500$ rpm.

To act as a generator, the machine must normally operate in the supersynchronous region, since the negative torque needed for generation is normally only realized in this region where the rotational speed is faster than the synchronous speed. If rotor is no longer short-circuited but supplied by a converter using a slip ring arrangement, control of the torque profile is possible. At a given wind speed, rotor current control permits optimal negative torque generation. Therefore, operation at the optimum rotational speed is achievable.

The power flow through the rotor converter is dependent on the slip of the machine as shown in Fig. 2(b). The slip is defined by

$$s = \frac{n_s - n_g}{n_s} \quad (4)$$

where n_g is the rotational speed of the machine. For supersynchronous operation (negative slip), power flows out of the rotor and for subsynchronous operation (positive slip) power is delivered to the rotor from the system. However, the net power flow out of the DFIG system is positive. The required operating speed range in the machine determines the slip range and consequently the rating of the rotor converter. Normally the system is designed to operate over a range of $s = \pm 33\%$. For such a case, the required rotor converter rating is 25% of the maximum power rating of the turbine.

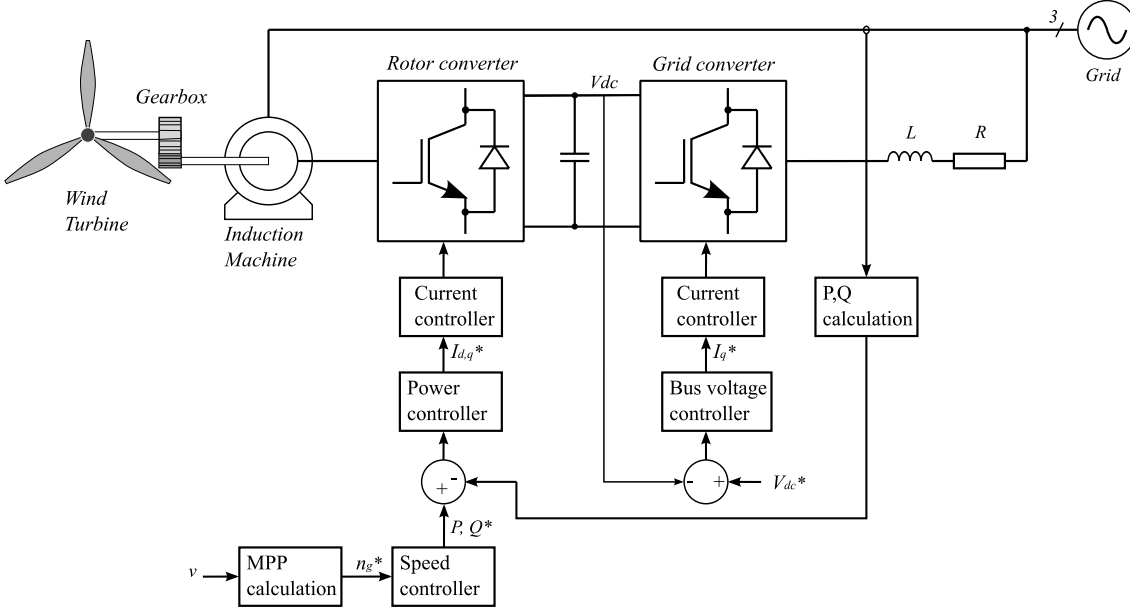


Figure 4: Block diagram of doubly-fed induction generator system.

3 Example DFIG System

The block diagram of the example DFIG system presented in the paper is shown in Fig. 4. The rotor supply circuit comprises a grid-side converter and rotor-side converter that are linked via a dc bus. The dc bus capacitor decouples the two converters, allowing them to be independently controlled. The parameters of the turbine and induction machine are given in Table. 1. The parameters have been adapted from a GE 1.5MW turbine [3]. It should be noted that the inertia was reduced by a factor of five in order to speed up the mechanical dynamic response of the turbine and allow for a faster simulation. This has a minor impact on the selection of parameters for the speed controller in the rotor-side converter control loop.

3.1 Grid Converter Control

The task of the grid side converter is to regulate the voltage of the dc bus, V_{dc} . To achieve this, a voltage control loop controls the d-axis current, I_d^* that affects the real power exported to or imported from the grid. The grid side converter can also be used for system power factor control by adding a reactive power control loop to control the q-axis current. In the example system, unity power factor operation is assumed and the q-axis current reference is therefore set to zero.

3.2 Rotor Converter Control

The the purpose of the rotor converter is to control the generator speed to achieve maximum power

Table 1: DFIG Turbine & Induction Machine Parameters

Rated power	P_m	1.5 MW
Rated voltage (line)	V_l	575 V
Frequency	f	50 Hz
Stator/rotor turns ratio	N	1
Stator resistance	R_s	0.0014 Ω
Rotor resistance	R_r	0.992 m Ω
Stator leakage inductance	$L_{s\lambda}$	89.98 μ H
Rotor leakage inductance	$L_{r\lambda}$	82.09 μ H
Magnetizing inductance	L_m	1.53 mH
Pole pairs	z_p	2
Bus capacitance	C	38 mF
Inertia	J	5 kg.m ²
Gearbox ratio	n	1:75.71
Turbine radius	R	35 m
Rated wind speed	v_{max}	12 m/s

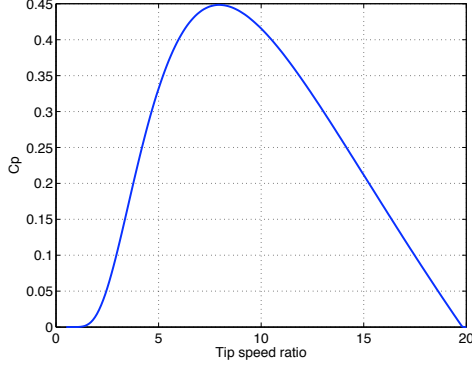


Figure 5: Wind turbine performance coefficient vs. tip speed ratio.

from the wind over a range of wind velocities. The rotor converter control scheme is based on a multi-tiered structure that comprises a speed, power and current control loop. It should be noted that omission of the power control loop is possible by implementing decoupled current control [4].

The reference speed for the outer speed control loop is determined by a maximum power point (MPP) calculation based on the wind velocity. Speed control is implemented by controlling the real power reference to the power control loop. In the power control loop, the reactive power reference is set to zero because it is assumed that the grid side converter will supply the needed reactive power to the system.

The current controller tracks the power reference by controlling the rotor currents. Current control is performed in a dq reference frame that is aligned with the position of the rotor.

4 System Modeling

The simulation model takes into account the dynamics of the wind turbine, the mechanical and electrical dynamics of the induction machine, and the electrical dynamics of the grid and rotor-side converters and dc bus. What is not taken into account are the slower dynamics of blade pitch control. It is therefore assumed that the blade pitch angle remains constant at 0° and the wind speed never exceeds the rated value of 12 m/s.

4.1 Wind Turbine Model

The wind turbine is modeled by converting the aerodynamic power created by the wind into a mechanical torque that drives the induction machine. The aerodynamic power, P_w , is calculated using Eq. (1) and the mechanical torque is calculated with

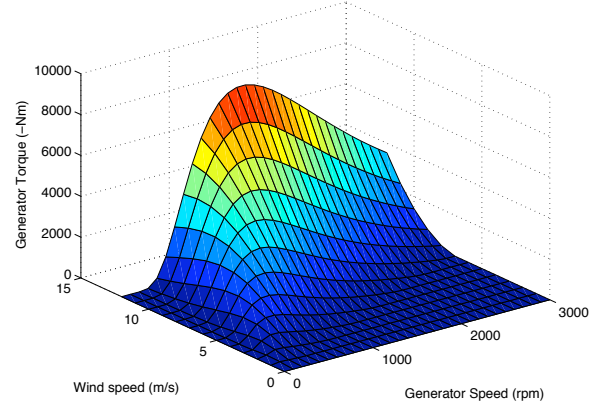


Figure 6: Wind turbine dynamics modeled as a torque surface.

$$T_m = -\frac{P_w}{\omega_t} \quad (5)$$

$$= -0.5\rho AC_p v^3 \frac{60n}{2\pi n_g} \quad (6)$$

where n is the gearbox ratio. The performance characteristic, C_p , is approximated with the following equation:

$$C_p = 0.244 \left(\frac{130}{\lambda} - 6.56 \right) e^{-13.3/\lambda} \quad (7)$$

The performance characteristic for the example wind turbine is shown in Fig. 5. It can be seen that an optimal C_p of 0.45 exists at the optimal tip speed ratio of 8.0.

The torque model of the turbine, calculated from Eq. (6), is dependent on two variables, v and n_g . When these parameters are swept over their operating range, the resultant torque characteristic is a surface, as shown in Fig. 6. For reasons of computational efficiency, the torque model of the wind turbine is implemented in the simulation model as a lookup table.

4.2 Induction Machine Model

The induction machine model is implemented using the standard PLECS library model of an induction machine with an open rotor. The electrical part of the machine is implemented as an equivalent dq model and the mechanical dynamics of the rotor are represented using

$$\dot{\omega} = \frac{1}{J}(T_e - F\omega_m - T_m) \quad (8)$$

where T_m is the external torque input from the wind turbine model, T_e is the electrical torque calculated in the electrical machine model, F is the co-

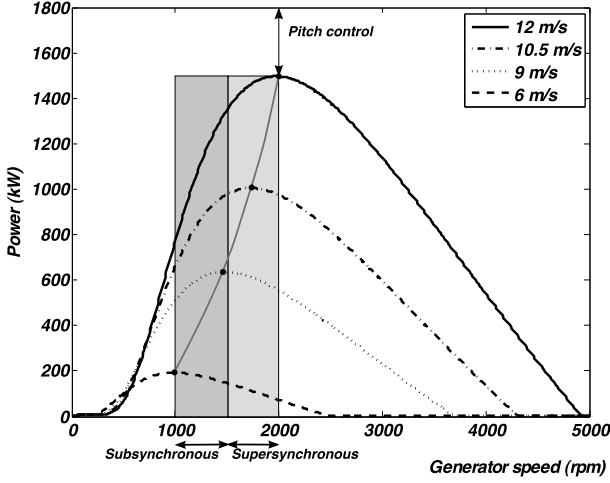


Figure 7: Output power graphs of the wind turbine showing the maximum power points for different wind speeds. Valid operating range of the simulation model is indicated by the shaded areas.

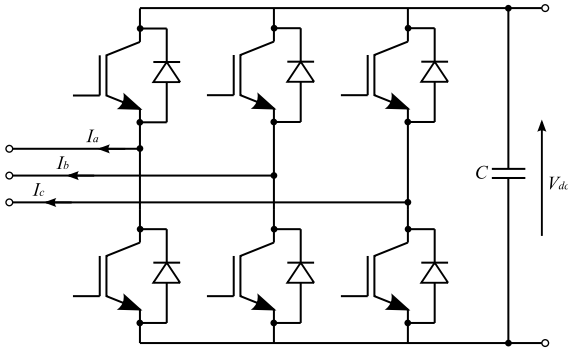


Figure 8: Switched PWM Converter Model.

efficient of friction and J is the combined inertia of the rotor and turbine.

4.3 Converter Model

Two different converter models are used in the simulation; a switched 3 phase PWM converter model shown in Fig. 8 and an averaged PWM converter model shown in Fig. 9. The switched model is used to simulate the fast electrical dynamics of the system and the averaged model idealizes the switching action, making it suitable for longer simulations in which the slower mechanical and wind speed dynamics are studied.

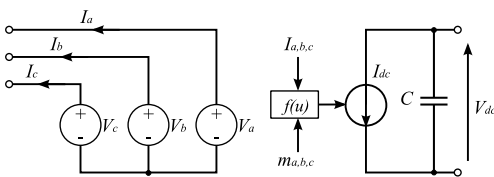


Figure 9: Averaged PWM Converter Model.

With the averaged PWM converter model, the assumption is that the PWM is ideally imposed. The ac-side voltages are therefore modeled as controlled voltage sources whose magnitude is calculated using

$$V_i = 0.5m_iV_{dc} \quad (9)$$

where m_i is the modulation index of each converter phase. The dc-side current is then calculated from the measured ac currents as follows:

$$I_{dc} = 0.5(m_aI_a + m_bI_b + m_cI_c) \quad (10)$$

4.4 Operating Range

The output power of the wind turbine that is calculated using Eq. (1) and (7) is shown in Fig. 7 as a function of wind speed and generator rotational speed. It can be seen that the maximum output power of 1.5 MW, generated at a wind speed of 12 m/s, is harnessed at a generator rotational speed of 2000 rpm. The wind turbine is not designed to produce a steady-state output of more the 1.5 MW. In practice, blade pitch control is used to reduce the aerodynamic power at higher wind speeds. Blade pitch control has been omitted from the turbine model since the focus of the simulation is on the faster electrical and motor dynamics. Therefore the model is only valid up to wind speeds of 12 m/s.

4.5 Maximum Power Tracking

In the example system, maximum power tracking is implemented using a simple technique that infers the optimal rotational speed of the generator, n_g^* , from the wind speed measurement, v . The relationship between optimal generator rotational speed in rpm and wind speed is given as follows:

$$n_g^* = \frac{60\lambda_{opt}n}{2\pi R}v \quad (11)$$

where n is the gearbox ratio.

4.6 Algebraic Loops

Algebraic loops are present in the DFIG system model that contains the averaged PWM converter model. The output states are directly dependent on the previous output due to the feedback-based control loops. This forces Simulink to solve each simulation time step iteratively, slowing down the simulation. Memory blocks or low-pass filters can be placed in the algebraic loop in order to rectify this problem. Since the simulation is configured for variable time step simulation, low-pass filters are used to break the algebraic loop. Low-pass filters produce more deterministic behaviour than a memory block in a variable-step environment.

5 Running the Simulation

Two simulation models are included in the example package. One model is based on switched PWM converter models and the other on averaged PWM converter models. Both examples have identical system parameters to allow for a direct comparison of results.

The system parameters can be found in the *.m* Matlab files that are supplied with the Simulink *.mdl* files. The *.m* function is automatically executed when the simulation is started. The name of the *.m* function can be found in the simulation model file under File > Model Properties > Callbacks > InitFcn. The simulation start and stop time and the induction machine parameters are specified and the wind turbine torque lookup table is initialized with data from the file *TmLookupData.mat*.

Running the simulation will initialize the DFIG system to run at a steady state operating point for a wind speed specified by the variable *Vw1* in the *.m* initialization function. The magnitude and time of the step change are also specified in the initialization function. The steady state operating point is imposed by loading an initial condition vector and applying the values to the integrators in the control loops and the parameters of the induction machine. A step change in wind speed can be applied to the turbine to observe the operation of the system in response to such a disturbance.

The example simulation models are configured to show the effect of a step change in wind speed from 12 m/s to 10.5 m/s or from 10.5 m/s to 8 m/s. With a wind speed of 12 m/s the total output power of the system is 1.5 MW, and the generator rotational speed is 2000 rpm. Reducing the wind speed to 10.5 m/s causes the output power to decrease to 1 MW and the optimal generation speed to decrease to 1750 rpm. These operating points corresponds to the output power graph shown in Fig. 7. It should be noted that when the wind speed is decreased from 10.5 m/s to 8 m/s, the slip direction changes and consequently the rotor converter begins supplying power to the generator in order to permit generation in the subsynchronous region.

6 Conclusion

In this report, a combined electrical-mechanical simulation model of a DFIG system has been presented. The model includes all electrical details of the rotor side converters and induction machine and the mechanical dynamics of the rotor and wind turbine. The wind turbine is modeled using a unique torque model. Two models are included in the example package. One model, implementing full PWM switching is useful for examining the operation of the system down to the switching level. The second model, based on average PWM converter models, is an order of magnitude faster than the full switching model and is suitable for longer simulation runs where slower dynamics such as the mechanical performance and maximum power point tracking operation are studied.

References

- [1] F. Blaabjerg and Z. C. and S. Kjaer, "Power electronics as efficient interface in dispersed power generation systems," *IEEE Transactions on Power Electronics*, vol. 19, pp. 1184–1194, Sept 2004.
- [2] S. Muller, M. Deicke, and R. D. Doncker, "Doubly fed induction generator systems for wind turbines," *IEEE Industry Applications Magazine*, vol. 8, pp. 26–33, June 2002.
- [3] N. Miller, W. Price, and J. Sanchez-Gasca, "Dynamic modeling of ge 1.5 and 3.6 wind turbine-generators," tech. rep., GE Power Systems Energy Consulting, 2003.
- [4] R. Pena, J. Clare, and G. Asher, "Doubly fed induction generator using back-to-back pwm converters and its application to variable-speed wind-energy generation," *IEE Proceedings Electric Power Applications*, vol. 143, pp. 231–241, May 1996.